

FRACTIONAL WAVELET TRANSFORM PHASE FOR IRIS IMAGE KEY POINTS MATCHING

M. A. Protsenko¹, E. A. Pavelyeva²

¹ Faculty of Computational Mathematics and Cybernetics, Lomonosov Moscow State University, 119991, Russia, Moscow, Leninskie Gory, MSU – ma.protsenko@mail.ru

² Faculty of Computational Mathematics and Cybernetics, Lomonosov Moscow State University, 119991, Russia, Moscow, Leninskie Gory, MSU - pavelyeva@cs.msu.ru

Commission II, WG II/8

KEY WORDS: Fractional Fourier transform, Fractional wavelet transform, phase, biometrics, iris recognition, key points, image matching.

ABSTRACT:

In this article the fractional phase congruency method for iris image key points descriptors is proposed. The fractional phase congruency is calculated using fractional wavelet transform through the fractional Fourier transform. Fractional Fourier transform is the generalization of the classical Fourier transform. The use of fractional phase congruency can achieve better results compared to the use of the classical phase congruency. The comparison between phase congruency and fractional phase congruency for biometric iris images is given. The optimal parameters of fractional wavelet transform for iris image key points matching are found. The experimental results of the proposed method using the images from CASIA-IrisV4-Interval database are demonstrated.

1. INTRODUCTION

The Fractional Fourier transform is the generalization of the classical Fourier transform. (Namias, 1980). The fractional Fourier transform (FRFT) can be considered as a signal rotation in the time-frequency plane for a given angle. FRFT can be used in various signal processing problems (Gomez-Echavarría, 2020, Sejdic, 2011) and can also be effectively used in neural networks (Zhang, 2021, Sahinuc, 2022). The fractional Fourier image transformer can extract both global and local contexts effectively (Zhao, 2022). The fractional operations like fractional convolution (Mustard, 1998), fractional correlation (Mendlovic, 1995) can also be considered as a generalization of classical operations. Some fractional operations can help to obtain better results than classical methods (Protsenko, 2022).

Phase information is used in various signal processing algorithms. For example, phase based algorithms can be used for image edge (Asghari, 2015) and corner detection (Kovesi, 2003), image fusion (Zhu, 2019), image registration (Yu, 2020), image segmentation (Belaid, 2010), etc. The phase can be used for image quality assessment (Zhang, 2011, Wang, 2003). Phase information is often used in biometrics: in iris recognition (Daugman, 2009), face recognition (Chan, 2012), for finger knuckle pattern authentication (Hammouche, 2020), gait recognition (Rida, 2016), for fake biometric data detection (Saratxaga, 2016). The phase information is also used in convolutional neural networks as input data (Qi, 2021) or for data augmentation (Chen, 2021).

Phase congruency is used in many problems of image processing (Pavelyeva, 2018). In phase congruency method the signal wavelet transform with different values of scale parameter is calculated, and the points of similar phase values over all scales are used for image features detection (Kovesi, 2003). Using the fractional wavelet transform instead of the classical wavelet transform the fractional phase congruency method is obtained. The fractional wavelet transform is calculated using FRFT (Mendlovic, 1997). Since FRFT contains the information about the signal both in spatial and frequency domains the proposed fractional phase congruency method can give better results than the classical phase congruency method.

In this article the fractional phase congruency method for iris image key points matching is proposed. The iris is one of the most reliable human biometrics. Iris images contain a lot of unique patterns, and the most informative iris image features can be found as iris image key points. The key points are found using Hermite functions (Pavelyeva, 2013) and the key points descriptors are based on fractional phase congruency.

This paper is arranged as follows: in Section 2 the fractional Fourier transform and fractional wavelet transform are described. Sections 3 and 4 show the properties of fractional Fourier and fractional wavelet transforms phase. In Section 5 the fractional phase congruency method is proposed. Section 6 describes the iris key points descriptors. The experimental results are shown in Section 7. Finally, Section 8 provides some conclusions.

2. FRACTIONAL FOURIER AND WAVELET TRANSFORMS

The Fractional Fourier Transform (Namias, 1980) provides a family of linear transforms for each value of $a \in R$. The FRFT of order a converts the signal $f(x)$ to the complex signal $F(\lambda)$:

$$F^a[f(x)] = F(\lambda) = \int_{-\infty}^{\infty} f(x)K_a(x, \lambda)dx,$$

$$K_a(x, \lambda) = \begin{cases} \frac{1}{\sqrt{2\pi}}\sqrt{1-ictg\alpha} \exp\left(\frac{i(x^2 + \lambda^2)}{2}ctg\alpha - \frac{ix\lambda}{\sin\alpha}\right), & \alpha \neq \pi n \\ \delta(x - \lambda), & \alpha = 2\pi n \\ \delta(x + \lambda), & \alpha = \pi + 2\pi n \end{cases}$$

where $\alpha = a\pi/2$.

It can be seen that $F^a[f(x)] = F^{a+4}[f(x)]$, $a \in R$. FRFT can be considered as a signal rotation in the time-frequency plane for a given angle α (Fig. 1). Consider some special cases of the value α . When $\alpha = \pi/2$, then $a = 1$, and FRFT becomes classical Fourier transform. When $\alpha = 0$, then $a = 0$ and $F^0[f(x)]$ reduces to the identity operator. When $\alpha = -\pi/2$, then $a = -1$, and the FRFT is the inverse Fourier transform.

The different fractional Fourier transform properties, such as the rules of multiplication, division, integration, differentiation,

convolution and the methods for the discrete fractional Fourier transform calculation are described in (Saxena, 2005).

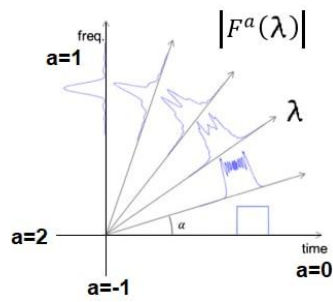


Figure 1: The illustration of fractional Fourier transform.

The fractional Fourier transform can be generalized to the two-dimensional case (Pei, 1998):

$$F^{a,b}[f(x,y)] = F(\lambda, \mu) = \int_{-\infty}^{\infty} \int_{-\infty}^{\infty} f(x,y) K_{a,b}(x,y,\lambda,\mu) dx dy,$$

$$K_{a,b}(x,y,\lambda,\mu) = K_a(x,\lambda) K_b(y,\mu).$$

The fractional wavelet transform is a generalization of the classical wavelet transform (Mendlovic, 1997). The classical wavelet transform is calculated by the formula:

$$W(s,p) = \int_{-\infty}^{\infty} f(x) G_{s,p}^*(x) dx,$$

where $G_{s,p}(x) = \frac{1}{\sqrt{s}} G\left(\frac{x-p}{s}\right)$, and $G(x)$ is the mother wavelet function, $s \in R^+$ is the scale parameter, $p \in R$ is the shift parameter.

The fractional wavelet transform is defined as

$$W_a(s,p) = \int_{-\infty}^{\infty} \int_{-\infty}^{\infty} K_a(x,\lambda) f(x) G_{s,p}^*(\lambda) dx d\lambda.$$

To calculate the fractional wavelet transform of order a in practice we perform the classical wavelet transform to the fractional Fourier transform of the required order a (Mendlovic, 1997). The fractional wavelet transform $W_{a,b}(s,p,q)$ can be generalized to the two-dimensional case (Kaur, 2023). To do this, we calculate the two-dimensional fractional Fourier transform $F^{a,b}[f(x,y)]$, and then we calculate the two-dimensional wavelet transform for the obtained result. In this article we use the parameters $a = b$, so we denote $W_{a,a}(s,p,q)$ as $W_a(s,p,q)$.

3. FRACTIONAL FOURIER TRANSFORM PHASE

The phase of Fourier transform contains information about the edges of image. For the fractional Fourier transform, a different amount of information about the edges can contain both the phase and the magnitude, depending on the value of the parameter a . It can be shown by FRFT phase and FRFT magnitude synthesis (Protsenko, 2022).

Let us take two images Lena and Baboon (Fig. 2) and combine the FRFT phase from one image and FRFT magnitude from another image (Fig. 3).



Figure 2: Lena and Baboon original images.

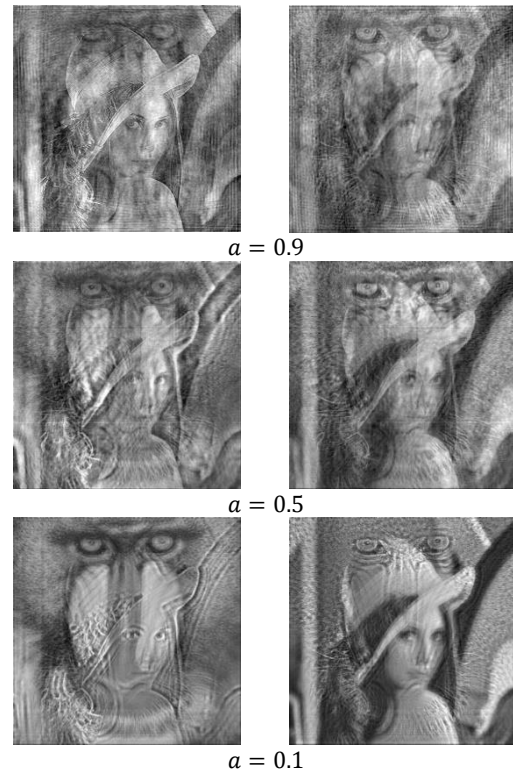


Figure 3: Synthesis of the FRFT phase and FRFT magnitude of different images. Left column images contain FRFT phase of Lena image and FRFT magnitude of Baboon image, and the right column, vice versa, FRFT phase of Baboon image and FRFT magnitude of Lena image.

If $|a|$ is close to 1, then FRFT phase contains more information about the image than the FRFT magnitude. When a is close to 0 the phase contains less information about the image, but the most high frequency information about the image edges remains. The obtained synthesis results show that FRFT contains the information about the image edges both in the phase and magnitude.

4. FRACTIONAL WAVELET TRANSFORM PHASE

The phase values of wavelet transform have a small difference over all scales s at feature points of the signal (Kovesi, 2003), that can be demonstrated using the phase scalogram. The phase scalogram shows the phase values for various values of the scale parameter s , the phase is mapped from 0-360 degrees to 0-255 gray levels for visualization.

We calculate the fractional wavelet transforms with different values of order a for different scale values s . Fig. 4 shows the example of a signal and its fractional wavelet transform phase scalograms: equal phase values are shown by equal colours; the vertical axis is the s -axis (directed down). The Gabor mother wavelet was used for the results in Fig. 4 and Fig. 5. Note that for $a = 0$ the result corresponds to the classical wavelet transform phase scalogram. We can see that if the signal has a feature point, then the phase of wavelet transform is invariant to the scale changes s at this point. This property is preserved using small a values, however, as a increases, the scalogram becomes less informative and this property disappears.

For the next example we consider the input signal with noise and its fractional wavelet transform phase scalograms (Fig. 5). The localization of noisy signals features can also be determined from the scalogram for the parameter a close to zero.

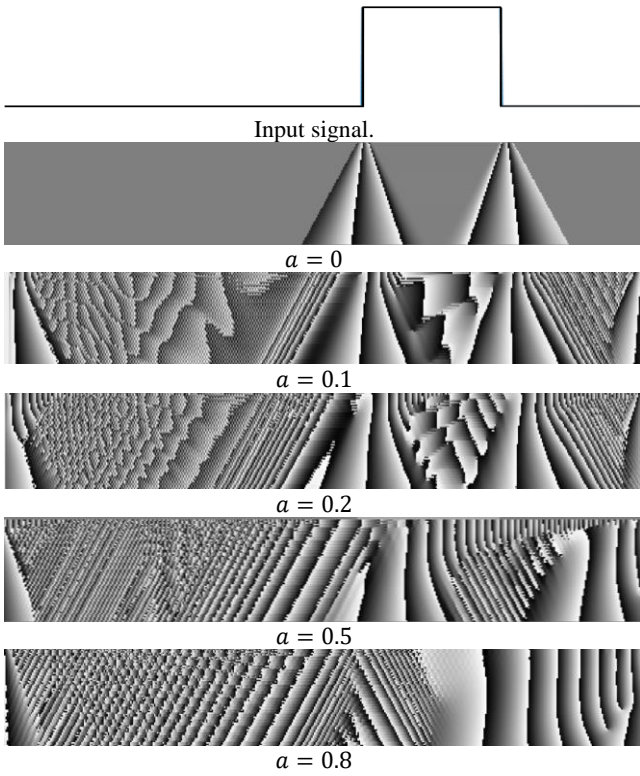


Figure 4: Phase scalograms of input signal with different values of order a .

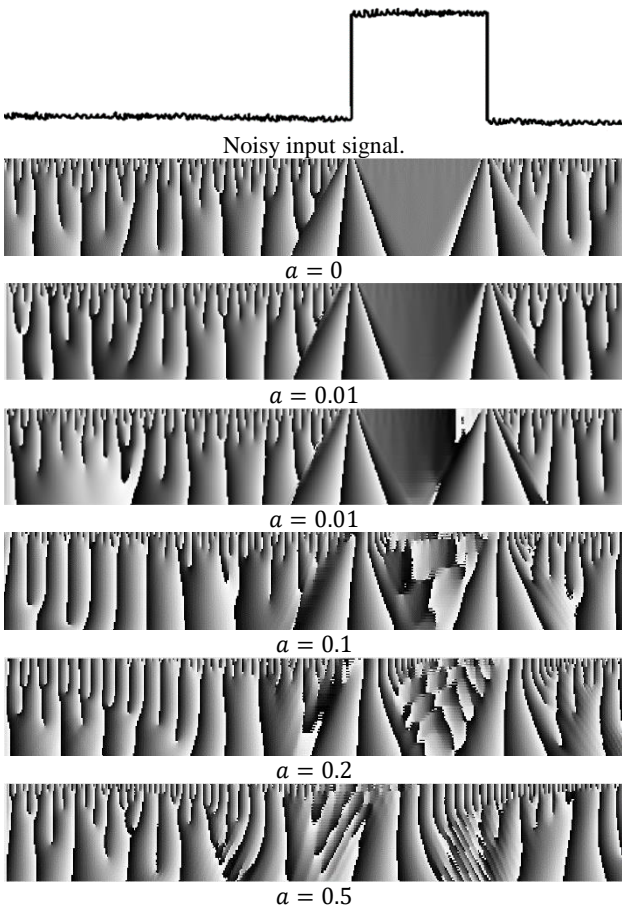


Figure 5: Phase scalograms of input signal with different values of order a .

5. FRACTIONAL PHASE CONGRUENCY

The phase congruency can measure the image features significance. Phase congruency provides a measure that is independent overall signal magnitude. So it is invariant to variations in image illumination and contrast (Kovesi, 2003).

The fractional phase congruency value at a point p we define in the analogy of classical phase congruency:

$$PC_a(p) = \frac{|\sum_s W_a(s, p)|}{\sum_s |W_a(s, p)| + \varepsilon}$$

ε is incorporated to avoid division by zero.

Let $W_a(s, p, q) = W_{a,a}(s, p, q)$ be the two-dimensional fractional wavelet transform. For two-dimensional case the log-Gabor wavelet function is used, and the two-dimensional wavelet transform is calculated using the convolution theorem. The taken parameters of log-Gabor function are described in (Protsenko, 2019). Six orientations and four scales of log-Gabor functions are taken. The two-dimensional fractional phase congruency value at a point (p, q) is defined as

$$PC_a(p, q) = \frac{\sum_\theta |\sum_s W_a(s, p, q)|}{\sum_\theta \sum_s |W_a(s, p, q)| + \varepsilon}$$

We take $\varepsilon = 0.001$ in the experiments. The fractional phase congruency visualization for different values of parameter a for square image is shown in Fig. 6. Note that for $a = 0$ the result corresponds to the classical phase congruency method.

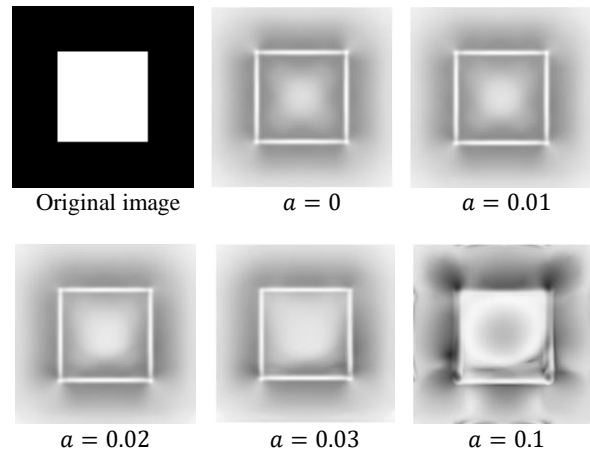


Figure 6: Phase congruency for the square image.

We can see that the fractional phase congruency with the parameter a close to zero contains the information about edges and corners of the original image. Moreover, the fractional phase congruency maps with $a = 0.01$ and $a = 0.02$ have more bright edges than the fractional phase congruency map with $a = 0$. If the parameter a is not close to zero and increases the edges disappear. The images in Fig. 6 show that the fractional phase congruency measure can find the image features of the original image with the parameter a close to zero.

6. IRIS KEY POINTS DESCRIPTORS

For iris image key points matching based on fractional phase congruency the iris images from CASIA-IrisV4-Interval database (CASIA, 2010) are used. After iris localization the images are normalized to a rectangular image size 512×64 (Fig. 7). In this work only $\frac{3}{5}$ part of the height of the initial normalized image (closer to the iris pupil) is taken as the normalized iris image since the areas around iris pupil have more sharp iris texture in the taken iris image database. The iris areas

free from the eyelashes, eyelids and glares are found (Tikhonova, 2020). Then the image contrast enhancement is applied.

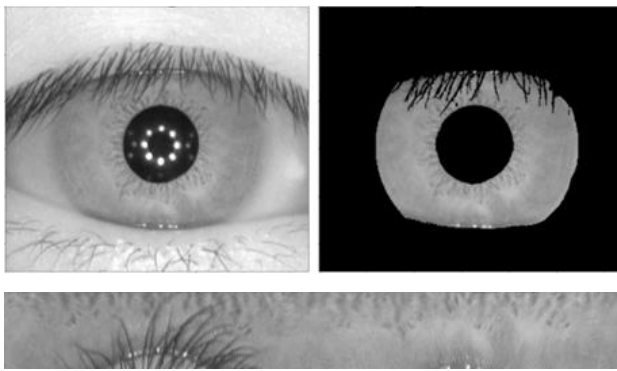


Figure 7: The iris image, iris segmentation and iris normalization results.

Fig. 8 shows the examples of iris image fractional phase congruency with different values of parameter a .

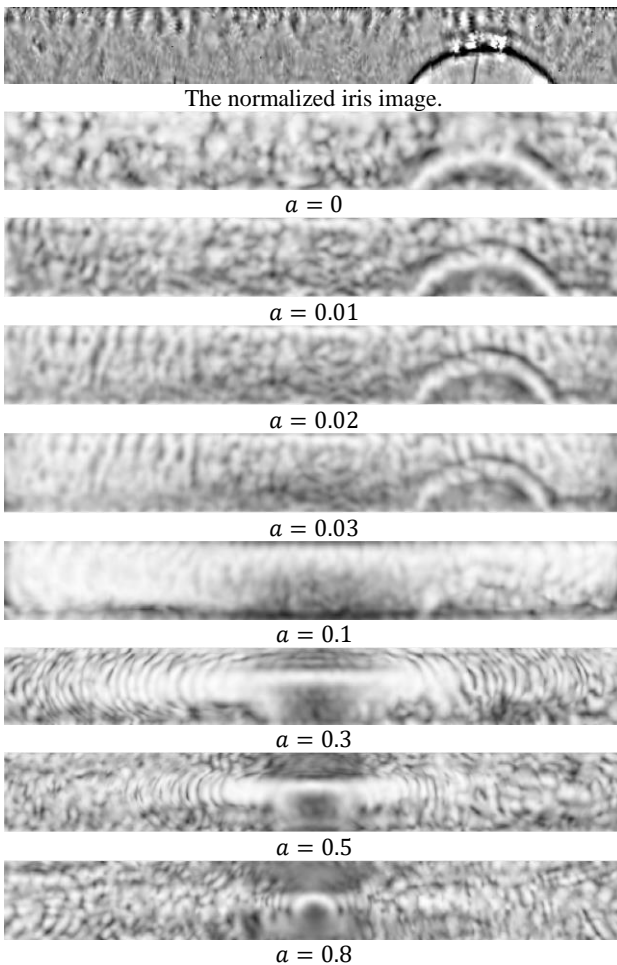


Figure 8: Iris image fractional phase congruency measures.

We see again that the values of parameter a close to zero can give us the information about iris image features so further we will use $a \in \{0, 0.01, 0.02, 0.03\}$.

For the normalized iris image the iris key points are found using the Hermite functions (Pavelyeva, 2013, Protsenko, 2019). Then we construct the iris key points descriptors using the fractional phase congruency. The descriptor is a feature vector that contains 25 fractional phase congruency values. One from key point and

next 24 from the points located on two concentric circles with the radiuses r and $2r$ around the key point, where $r = 3$.

If (x_0, y_0) are the key point coordinates, then the points where we need to calculate the fractional phase congruency values have the following coordinates:

$$x_1 = x, y_1 = y$$

$$x_i = x + r \cos\left(\frac{j\pi}{4}\right), y_i = y + r \sin\left(\frac{j\pi}{4}\right), j = 0..7, i = j + 2$$

$$x_i = x + 2r \cos\left(\frac{j\pi}{8}\right), y_i = y + 2r \sin\left(\frac{j\pi}{8}\right), j = 0..15, i = j + 10$$

The taken points are shown in Fig. 9. For better view only a part of normalized iris image is shown.

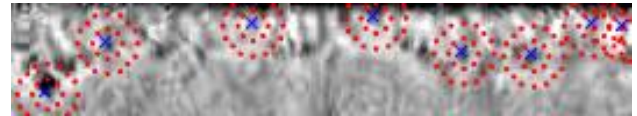


Figure 9: Some iris image key points (blue crosses) and points around them that are used to calculate the iris image key point descriptor.

To compare the key points, Euclidean metric between the feature vectors is calculated. Points outside the image have zero values, and these points are not used in Euclidean metric. To obtain the final result we divide the derived distance to the number of the used values. Thus the distance between two comparable key points P_1 and P_2 with the feature vectors $a = (a_1, \dots, a_{25})$ and $b = (b_1, \dots, b_{25})$ is

$$dist(P_1, P_2) = \frac{\sum_{i \in I} (a_i - b_i)^2}{|I|}$$

where $I = \{i \in \{1..25\}: a_i \cdot b_i \neq 0\}$.

If the distance between the key points of two iris images is less than a given threshold, then these key points are considered as belonging to the same iris texture area. We assume that the spatial shift between the comparable key points may correspond to the angle of eye rotation no more than ~ 20 degrees. So only key points $P_1 = (x_1, y_1)$ and $P_2 = (x_2, y_2)$ where the distance between x_1 and x_2 is no more than 30 pixels (taking into account the cyclic shift of the normalized iris image) and $|y_1 - y_2| \leq 5$ can be matched. Then we find the most frequent horizontal shift between the matched key points – this shift determines the global shift between normalized iris images and the rotation angle between the eyes. Knowing the global shift between normalized iris images we then allow the final horizontal shift between the key points no more than global shift plus or minus 5 pixels.

7. EXPERIMENTS RESULTS

The proposed method of iris image key points matching based on fractional phase correlation was tested with a part of CASIA-IrisV4-Interval database. The different values of order a were taken.

The distance between the iris images is equal to the number of matched iris key points. The distribution of genuine and impostor scores for different a is demonstrated in Fig. 10. Green lines correspond to genuine pairs comparison and red lines correspond to impostor pairs. The horizontal axis shows the number of matched pairs. The vertical axis shows the percentage of images for which a given number of matches were obtained.

We can see that the results for $a = 0.01$ and $a = 0.02$ are better than for $a = 0$. The distributions for $a = 0.02$ are the most separated. It means that the fractional phase congruency in iris key points descriptor based on classical phase congruency ($a = 0$) can be improved by using fractional phase congruency with $a = 0.02$.

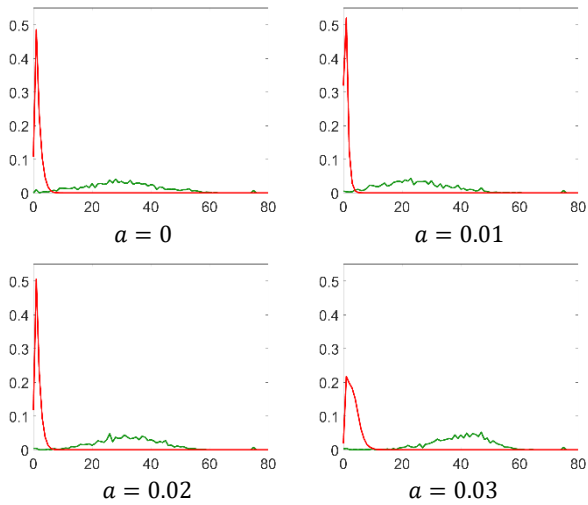


Figure 10: The genuine (green line) and impostor (red line) distribution scores for different values of order a .

The examples of iris key points extraction and key points matching for two images of one eye for different values of order a are shown in Fig. 11, Fig. 12 and Fig. 13. The red lines connect the matching key points. Blue dots show the iris image key points. Fig. 12 and Fig. 13 show the examples where small numbers of matched key points were found with $a = 0$ but the algorithm found more corresponding key points for $a = 0.02$ and $a = 0.03$. The example of iris key points matching for two images of different eyes is shown in Fig. 14.

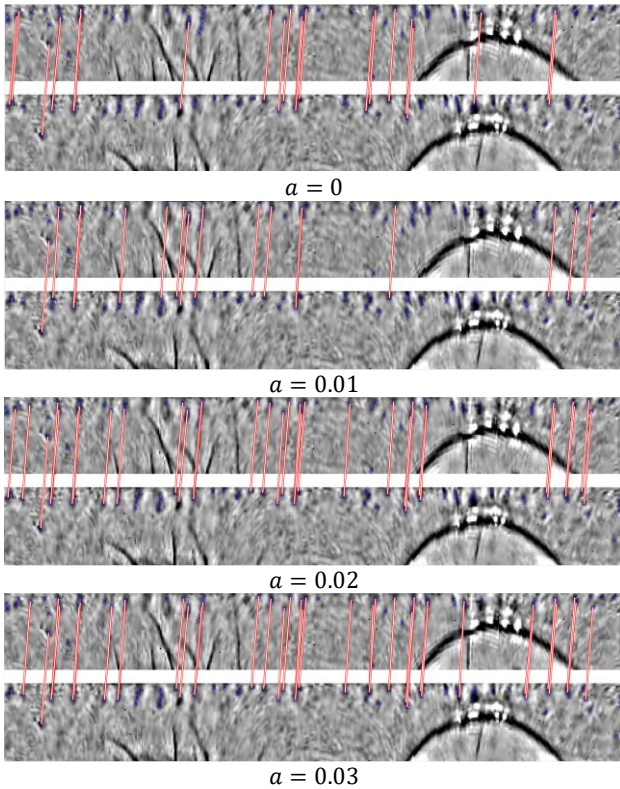


Figure 11: The examples of key points matching for two iris images of one eye.

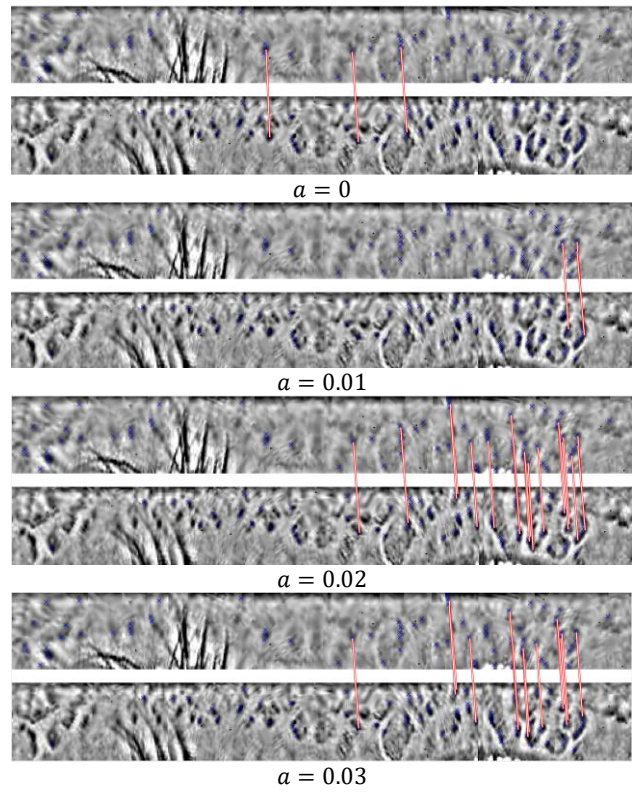


Figure 12: The examples of key points matching for two iris images of one eye.

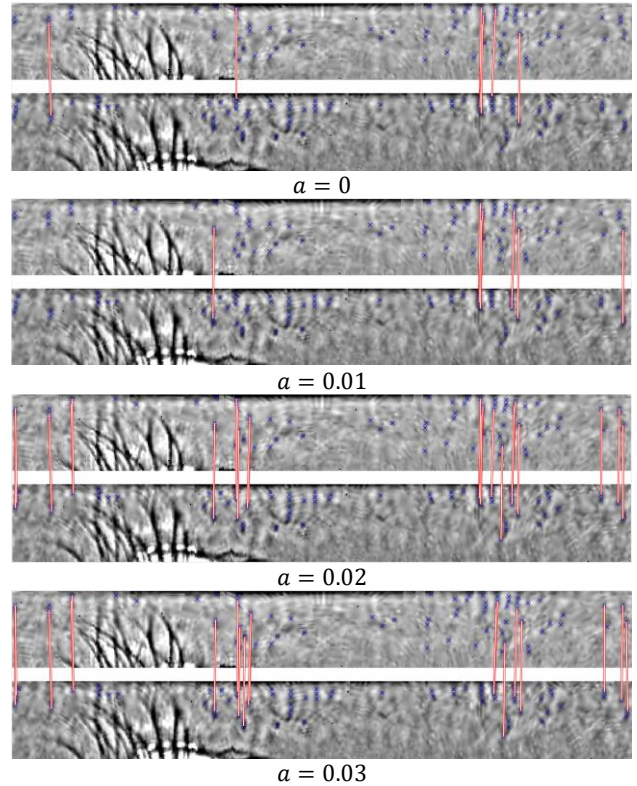


Figure 13: The examples of key points matching for two iris images of one eye.

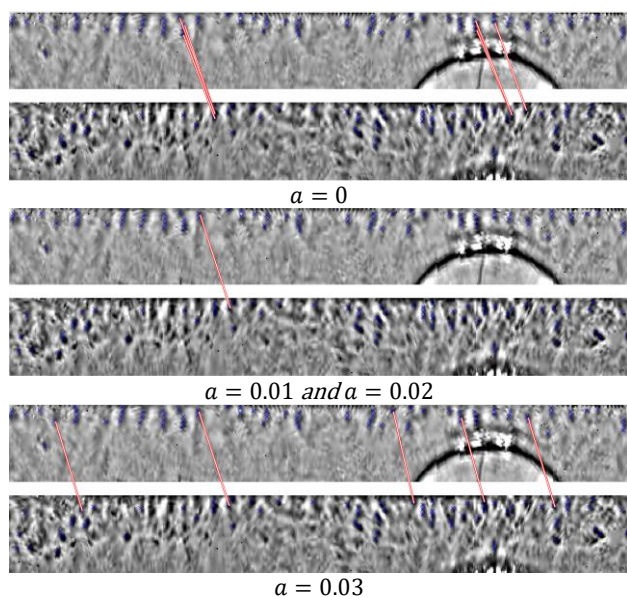


Figure 14: The example of key points matching for two iris images of different eyes.

8. CONCLUSION

In this article the iris image key points matching method based on fractional phase congruency is proposed. The iris image key points are calculated using the Hermite functions. The fractional wavelet transform in iris key points is calculated to obtain the iris image key points descriptors. The fractional phase congruency is compared to the classical phase congruency for iris image key points matching. The selection of optimal parameter for fractional phase congruency function is proposed. The results show that the use of fractional phase congruency method can be promising in image analysis and biometrics.

REFERENCES

- Asghari M. H., Jalali B., 2015. Edge detection in digital images using dispersive phase stretch transform. In: International journal of biomedical imaging, Vol. 2015, pp. 1-6.
- Belaid A., 2010. Phase-based level set segmentation of ultrasound images. In: IEEE Transactions on Information Technology in Biomedicine, Vol. 15, № 1, pp. 138-147.
- Chan C. H., 2012. Multiscale local phase quantization for robust component-based face recognition using kernel fusion of multiple descriptors. In: IEEE Transactions on Pattern Analysis and Machine Intelligence, Vol. 35, № 5, pp. 1164-1177.
- Chen G., 2021. Amplitude-phase recombination: Rethinking robustness of convolutional neural networks in frequency domain. Proceedings of the IEEE/CVF International Conference on Computer Vision, pp. 458-467.
- Daugman J., 2009. How iris recognition works. The essential guide to image processing. In: Academic Press, pp. 715-739.
- Gomez-Echavarria A., Ugarte J. P., Tobon C., 2020. The fractional Fourier transform as a biomedical signal and image processing tool: A review. In: Biocybernetics and Biomedical Engineering 40.3, pp. 1081-1093.
- Hammouche R., Attia A., Akrouf S., 2020. A novel system based on phase congruency and gabor-filter bank for finger knuckle pattern authentication. In: ICTACT J Image Video Process, Vol. 10, № 3, pp.2125-2131.
- Kaur N., Gupta B., Verma A. K., 2023. Multidimensional fractional wavelet transforms and uncertainty principles. In: Journal of Computational and Applied Mathematics, pp. 115-250.
- Kovesi P., 2003. Phase congruency detects corners and edges. In: The Australian pattern recognition society conference: DICTA, Vol. 2003, pp. 309–318.
- Mendlovic D., Ozaktas H. M., Lohmann A. W., 1995. Fractional correlation. In: Applied Optics, Vol. 34, № 2, pp. 303-309.
- Mendlovic, David, 1997. Fractional wavelet transform. In: Applied optics 36.20, pp. 4801-4806.
- Mustard D., 1998. Fractional convolution. In: The ANZIAM Journal, Vol. 40, № 2, pp. 257-265.
- Namias V., 1980. The fractional order Fourier transform and its application to quantum mechanics. In: IMA Journal of Applied Mathematics, Vol. 25, № 3, pp. 241-265.
- Pei S. C., Yeh M. H., 1998. Two dimensional discrete fractional Fourier transform. In: Signal Processing, Vol. 67, № 1, pp. 99-108.
- Pavelyeva E. A., 2013. The search for matches between the iris key points using Hermite projection phase-only correlation method. In: Systems and Means of Informatics, 23(2), pp. 74-88 [In Russian].
- Pavelyeva E. A., 2018. Image processing and analysis based on the use of phase information. In: Computer Optics, 42(6), pp. 1022-1034.
- Protsenko M. A., Pavelyeva E. A., 2019. Iris Image key points descriptors based on phase congruency. In: The International Archives of the Photogrammetry, Remote Sensing and Spatial Information Sciences, Vol. 42, pp. 167-171.
- Protsenko M. A., Pavelyeva E. A., 2021. Image key point matching by phase congruency. In: Computational Mathematics and Modeling, Vol. 32, № 3, pp. 297-304.
- Protsenko M. A., Pavelyeva E. A., 2022. Fractional Fourier Transform Phase for Image Matching. In: Graphicon-Conference on Computer Graphics and Vision, Vol. 32.
- Tikhonova V. A., Pavelyeva E. A., 2020. Hybrid iris segmentation method based on CNN and principal curvatures. In: CEUR Workshop Proceedings, Vol. 2744, № 31, pp. 1-10.
- Qi X., 2021. Chest X-ray image phase features for improved diagnosis of COVID-19 using convolutional neural network. In: International journal of computer assisted radiology and surgery, Vol. 16, pp. 197-206.
- Rida I., Almaadeed S., Bouridane A., 2016. Gait recognition based on modified phase-only correlation. In: Signal, Image and Video Processing, Vol. 10, № 3, pp. 463-470.
- Sahinuc F., Koç A., 2022. Fractional Fourier transform meets transformer encoder. In: IEEE Signal Processing Letters, Vol. 29, pp. 2258-2262.

Saratxaga I., 2016. Synthetic speech detection using phase information. In: *Speech Communication*, Vol. 81, pp. 30-41

Saxena, R., Singh, K., 2005. Fractional Fourier transform: A novel tool for signal processing. In: *Journal of the Indian Institute of Science*, Vol. 85, №. 1, pp. 11 - 26.

Sejdic E., Djurovic I., Stankovic L. J., 2011. Fractional Fourier transform as a signal processing tool: An overview of recent developments. In: *Signal Processing*, Vol. 91, №. 6, pp. 1351-1369.

Wang Z., Simoncelli E., 2003. Local phase coherence and the perception of blur. In: *Advances in neural information processing systems*, Vol. 16, pp. 1435-1442.

Yu G. and Zhao S., 2020. A new feature descriptor for multimodal image registration using phase congruency. In: *Sensors* 20.18, pp. 5105.

Zhang L., 2011. FSIM: A feature similarity index for image quality assessment. In: *IEEE transactions on Image Processing*, Vol. 20, №. 8, pp. 2378-2386.

Zhang L., Cheng B., 2021. Fractional Fourier transform and transferred CNN based on tensor for hyperspectral anomaly detection. In: *IEEE Geoscience and Remote Sensing Letters*, Vol. 19, pp. 1-5.

Zhao X., 2022. Fractional fourier image transformer for multimodal remote sensing data classification. In: *IEEE Transactions on Neural Networks and Learning Systems*, pp. 1-13.

Zhu, Z., 2019. A phase congruency and local Laplacian energy based multi-modality medical image fusion method in NSCT domain. In: *IEEE Access* 7, pp. 20811-20824.